Eur. Phys. J. B **42**, 435–440 (2004)
DOI: 10.1140/epjb/e2004-00401-9

THE EUROPEAN PHYSICAL JOURNAL B

Defects in nanocrystalline SnO_2 studied by Tight Binding

A.M. Mazzone[a] and V. Morandi

CNR-IMM, Via Gobetti 101, 40129 Bologna, Italy

Received 7 April 2004 / Received in final form 7 October 2004
Published online 23 December 2004 –

Abstract. In this work we present a study of the properties of defective nanostructures. The material chosen to this purpose, i.e. SnO_2, has practical applications and many of them rely on the spontaneous formation of vacancies. Therefore, crystalline grains with shape and size comparable to the experimental ones have been considered. According to the bulk properties, the grains lattice has the rutile structure and may also include vacancy defects. The calculations describe the effects of the structural grain parameters, i.e. size and shape, as well as of the defect type, on the grain cohesion and are based on a Tight Binding method. The comparison with Density Functional calculations, also carried out in the course of this study, illustrates the limits of both methods when used for these complex structures.

PACS. 61.46.+w Nanoscale materials: clusters, nanoparticles and nanocrystals – 31.10.+z Theory of electronic structure, electronic transitions and chemical bonding – 31.15.Ew Density functional theory

1 Introduction

Interest in the physical properties of structures of finite size has increasing in recent years and a broad literature is now available on clusters, nanowires, nanotubes and quantum devices. Major problems exist in the understanding of nanocrystalline materials. Published results, chiefly dealing with silicon and metals, indicate that the building blocks of these materials are formed by grains with thousands of atoms and nanometric dimensions. The assembling processes, though retaining the crystalline structure of the bulk phase, lead to grains with an irregular shape containing faulted growths, twined boundaries, disclinations and a defective stoichiometry in compounds. A central problem in nanoscience is to understand if these defects are structurally and energetically similar to the bulk ones and what are their possible effects on the stability and cohesion of the material, as well as on its transport and optical properties. While the answer to these questions require the concerted efforts of experimentalists and theoreticians, the problem is further complicated by the variety of nanocrystalline materials employed in current technologies.

Among the oxides in the rutile family, SnO_2 is of considerable technological interest owing to its application in heat-reflecting filters, as transparent electrodes in Si solar cells and as gas sensors. It is known that rutile is almost naturally reduced and multiple vacancies are generated even in a low-temperature treatment. This property is important for its application as a sensor of inflammable or poisonous gases. In fact the change of its oxygen content leads to a change of conductivity which can be detected by the use of a suitable circuit. For this application the nanocrystalline material, owing to the many percolative paths among grains, is better suited than the thick film. However, while many detailed theoretical studies are available for the bulk, very few works at a basic level have been dedicated to its nanocrystalline phase, in spite of the intensive experimental efforts.

This state of the art is not without ground. In fact, the rutile lattice of SnO_2 and its electronic configuration represent a severe test for computational methods regardless of their accuracy. Historically, the major chemical trends on bonding, impurity and vacancy levels in the main gap of the material and on vacancies at the surface, have been calculated at a semi-empirical level using the Tight Binding (TB) formulation. This in itself suggests that TB holds important potentialities for the characterization of the material and has motivated this work. The purpose of the present study is double. First, emphasis is given to the presence of stoichiometric defects. These, according to the properties of the bulk, have been assumed to be vacancies and we study the relationship between the grain size, shape and vacancy types and the properties of its electronic charge. From a methodological standpoint the characterization of even simple defects in a nanograin structure, such as the ones considered in this study, is a not trivial task owing to the absence of a band structure and formation energy. It will be shown that the binding energy is a simple and sufficiently accurate indicator of the desired relationship between the defect and the electronic charge in the grain. Second, elements with

[a] e-mail: mazzone@bo.imm.cnr.it

a high Z number are difficult to treat with current all-electron approaches, owing to the large number of electrons and of their correlations. For SnO_2 the problem is aggravated by the interactions between tin and oxygen. Therefore any computational method has to be viewed in light of the other, possibly more refined, approaches. Accordingly, two different approaches, i.e. Tight Binding and Density Functional Theory (DFT), have been adopted. Though the former one has been applied more extensively than the other one, their comparison illustrate the limits of both.

The paper is organized as follows. Sections 2 and 3 describe the TB and DFT methods and the structural models used in the calculations. TB calculations of the grains are reported in Section 4 whereas the comparison of DFT and TB is presented in Section 5.

Table 1. TB parameters [2]. Energies in eV. Distances in Å. All the energies are negative.

diagonal matrix elements					
symmetry	O			Sn	
s	29.2			11.3	
px	14.3			5.0	
py	14.1			5.0	
pz	14.2			5.0	
two-center interactions					
distance	$p\sigma$	$p\pi$	sp	ps	s
	O-O				
2.91	0.39	0.02			
3.19	0.23	0.008			
	Sn-O				
2.05	3.01	1.00			
2.59	0.70	0.05	2.85	2.02	1.58

2 TB and DFT methods

The TB approach lies between empirical potentials and more accurate all electron calculations. By bringing into play the electronic structure of the system, TB describes the quantum effects which are unvailable to empirical potentials. With respect to more accurate all electron calculations, its simple formulation allows one to treat systems containing thousands of atoms with modest computational efforts.

In the TB formulation the total energy of the system E_{tot} results from the sum of the kinetic energy of the atoms, of the band-structure energy E_{bs} and of an additional term E_{rep} [1]. While the first one is important in Molecular Dynamics for the evaluation of the lattice forces, the energetics of the system is determined by the other two. E_{bs} contains the one-electron energy spectrum and is obtained from a secular equation which linearly depends on the overlapping and one-electron matrices S and H, respectively. The energy E_{rep} contains ion-ion interactions and the parts of the Hartree, exchange and correlation energies which are not included into E_{bs}.

The main assumptions used for the evaluation of the quantities above can be summarized as follows:

(i) The matrix elements S_{ij} are calculated directly. Therefore their evaluation can be refined by the use of more complete basis sets as they become available. In the following calculations, the essential contributions to bonding, i.e. the s, p states of tin and the p states of oxygen, are all included.

(ii) The H parameterization at the nearest neighbour distance is based on [2] (the corresponding energies are reported in Tab. 1) and an extended connectivity from second- through to fourth-nearest-neighbours is also accounted for. For interactions beyond the nearest neighbour a d^{-n} scaling, with n equal to 2 or 5 for s, p and d orbitals, has been adopted. This allows one to account for the vanishing of the wave functions on the grain boundaries or in a vacant lattice site.

(iii) The interionic energy E_{rep} follows a power law in the interatomic separations such as:

$$E_{rep} = \sum_{ij} c_1 (r_{1,ij}/r_{1,0})^n + c_2 (r_{2,kl}/r_{2,0})^n \quad (1)$$

where $r_{1,0}$ and $r_{2,0}$ are the nearest tin-oxygen and oxygen-oxygen distances, respectively. $r_{1,ij}$ is the distance between tin atom i and oxygen atom j and $r_{2,kl}$ is the distance between oxygen atom k and l. The value of the constants n, c_1, c_2 is -14.696, 0.20059 and 0.000102 respectively. As also reported in [3], it has been found that the choice of these parameters is not critical and that the conditions (ii) and (iii) lead to a good fitting of the bulk band structure.

The TB method was developed on top of the package ICON [4] which includes a flexible definition of H and iterative techniques for the solution of the secular equation and for geometry optimization.

Density Functional calculations are based on SIESTA. SIESTA is a self-consistent Density Functional method (calculations using SIESTA are therefore indicated as DFT) employing standard norm-conserving pseudopotentials in their fully non local form, and a flexible linear combination of atomic orbitals for the description of the valence charge [5]. The electronic structure of tin and oxygen is $5s^2 5p^2$ and $2s^2 2p^4$, respectively. Both Local Density Approximation and Generalized Gradient Corrections have been used as exchange-correlation functionals. The pseudo-potentials follow the Troullier-Martins formulation with a cutoff radius equal to 1.2 a.u. (oxygen) and 1.9 a.u. (tin) and the tin potential may include scalar-relativistic corrections (a similar formulation has been also adopted in [6]). Other inputs of the calculations are single- and double-ζ basis sets plus polarization (indicated as SZ, DZ and SZP, DZP respectively) and a mesh cutoff of 80.0 Ry.

3 The structural models

Two types of structures are considered in the following calculations: i.e. small clusters formed by tin and oxygen, and nanocrystalline grains. The first ones are used to illustrate the general features of bonding in SnO systems, and as a simple benchmark of TB and DFT. Their structure is obtained from the minimization of the total energy E_{tot}. The second ones represent the nanocrystalline material. Owing to the size of the largest grains used in this study, the minimization of the total energy is not useful for the determination of their shape. For structures of this type, in fact, E_{tot} is a complex multivalue function with thousands of local minima of little physical significance. Any minimization procedure would be unavoidably trapped into one of these. The shape of the grains has therefore been constructed on the basis of the experimental data. X-ray observations [7,8] indicate that nanocrystalline materials with a fine grain structure retain the rutile structure of SnO_2. Device studies [9] show that, depending on the preparation techniques, the grain shape is columnar, or spongy, and the dimensions of the grains is in the range from 3 to 20 nm. Therefore two basic models of grains, spherical and columnar, with the rutile lattice of SnO_2, have been adopted in the following calculations (these grains are indicated below as S and C, respectively. These models are also used in previous studies [10,11]). The spherical structures, obtained by carving a sphere into a cubic box, represent the spongy clusters. The columnar grains are obtained by cutting the box parallel to the bulk (100) planes. The section of these grains is squared and their height can be elongated along the a or c direction. In the following, to simplify the notations, a and c indicate the grain dimensions along the a and c axes of the crystal. With this notation, an 'elongated grain' indicates a columnar grain with a ratio a/c in the range of 5–90, while this ratio is between 1.2–2.0 in the other cases. The grain size N varies from approximately 10 to 600 atoms with a linear dimension in the range of 0.4–3 nm. These dimensions are comparable with the smaller experimental values. Defects are produced by the removal of one atom in the oxygen or in the tin sublattice (these structures are indicated as 1OV and 1SnV, respectively). Test calculations on the defect location were performed at each size by displacing the vacancy from the grain center to its boundaries.

TB calculations were applied to grains of all sizes and shapes with a rigid lattice model. The DFT ones were limited to $N \leq 80$ and the lattice was relaxed to an energy minimum using conjugate gradients.

4 The properties of crystalline grains. The defective lattices

To set the stage briefly, it is recalled that SnO_2 belongs to the tetragonal crystal system and its lattice is shown in Figure 1. This presentation in itself explains the complex bonding network of this material. Atomic positions

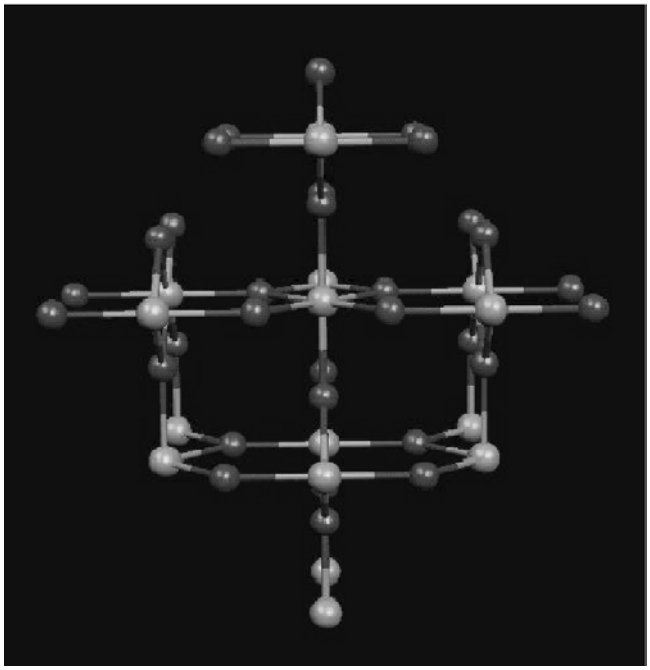

Fig. 1. The lattice structure of SnO_2. Tin and oxygen atoms are marked as light and dark grey, respectively.

are determined by the c/a ratio and by the internal parameter u. Experimental values of these parameters are $u = 0.3064$, $a = 4.737$ Å, $c/a = 0.6726$. Each tin atom has two oxygens at a distance $d_1 = \sqrt{2}ua$ and four at $d_2 = (2(1/2 - u)^2 + c/2a))^2]^{1/2}a$ (both distances are in the range 2.05 Å) and each oxygen is bonded to a tin atom in a planar trigonal configuration.

Early studies on SnO_2 were directed at the evaluation of the band structure of oxides in the rutile family [2,17,18], whereas the more recent ones have addressed the comparison between the tin oxides, SnO and SnO_2, and silicon oxides [6,19–24]. In agreement with experiments, these calculations show that SnO_2 exhibits a direct-forbidden gap. Its conduction band minimum is largely Sn s-like while its valence band maximum is O-like and is localized on the p_π states. Oxygen vacancies are the more common defects of bulk SnO_2 and produce a donor state at about 0.1 eV below the conduction band minimum [2].

Due to the many applications of SnO_2 as a gas sensor, its surfaces have been attentively investigated and several studies deal with the most stable of them, i.e. (111), (110) and (100). These studies are of central importance in the context of this study since the physics of nanograins is obviously closer to that of surfaces than to the bulk. TB calculations show surface states with the characteristics of a hybridization between tin s and oxygen p orbitals [3, 12]. In spite of the ionic character of the bonding, the rumpling of the surface is modest, between 0.1 and 1 Å, and is accompanied by a counter-rumple in the subsurface layers. These effects do not lower the energy of any surface state at any point in K space by more than 0.2 eV. Furthermore, in contradiction with known properties of TiO_2,

Table 2. Properties of small clusters. Literature results, TB and DFT calculations. The sources for oxygen and tin clusters are [25] and [26–28], respectively. The two energies E_c(SnO) and E_c(SnO_2) indicate the cohesive energy of the two crystalline oxides, SnO and SnO_2 [19]. The bracketed value of Sn_4 was obtained by a large shift of the tin parameterization.

cluster	structure	binding energy E_b [eV/atom]		bondlenght [Å]
		literature data		
	-	expt.	calc.	
SnO-crystal	layered	4.36(E_c)		-
SnO_2-crystal	tetragonal	4.91(E_c)		-
O_2	-	–2.61	–3.30	1.18 expt.,1.20 calc.
Sn_2	-	–1.61	–1.96, –1.44	2.70 expt.
Sn_3	-	-	–2.27	
Sn_4	rhombus (calc.)	–1.98	–2.74	-
		TB calculations		
O_2	-	–2.83		1.18
Sn_2	-	–1.41		2.72
Sn_3	triangle	–2.25		2.45
Sn_4	rhombus	–2.13(–2.78)		2.68
SnO	-	–2.46		2.20
SnO_2	linear	–2.81		2.08
		DFT calculations		
		GGC	LDA	
O_2	-	–3.20, –2.80	–3.66, –3.21	1.32
Sn_2	-	–2.26, –1.65	–2.33, –2.11	2.60
Sn_3	triangle	–3.24 –2.83	–3.77, –3.09	2.80
Sn_4	rhombus	–3.51, –2.51	–3.91, –2.91	2.93
SnO	-	–3.80, –2.65	–3.66, –3.10	1.85
SnO_2	linear	–3.60, –3.15	–3.90, –3.40	1.95

no band-gap states are generated by oxygen-deficient reconstructed surfaces. This is because a significant rehybridization of the surface atoms is prevented by the large surface topology.

The data in Table 2 report the binding energy E_b of small oxygen and tin clusters. It is underlined that the energy E_b is the total energy E_{tot} measured with respect to an ensemble of free atoms of the same size and composition as the cluster. It is therefore indicative of the entire eigenvalue spectrum without the resolution into orbital components. However, as for the cohesive energy of the solids, E_b has a practical content and shows the stability against the dissolution into separate atoms. The comparison of E_b with the cohesive energy E_c of the two crystalline oxides, SnO and SnO_2, shows a perceptible reduction of the binding strength and a remarkable dependence of E_b on the cluster size and composition. In fact, the shape and binding energy of the Sn_n clusters are similar to the ones of silicon clusters [13], which indicates the formation of covalent bonds. A much stronger binding strength and shorter bonds are observed for O_n. The first of these properties is also observed for SnO_n whose bondlenght is however similar to the ones of Sn_n. These features suggest a mixed covalent-ionic charge for the SnO_n clusters.

The properties of the grains are illustrated in Figure 2. The figure shows plots of E_b-vs.-N in the various families of grains and a comparison is also made between the grains without and with vacancies. In agreement with the properties of small clusters, the binding strength is perceptibly lower than the cohesive energy in the solid and, as already reported in [10,11], there are also evident effects of the grain shape. For columnar grains with low a/c,

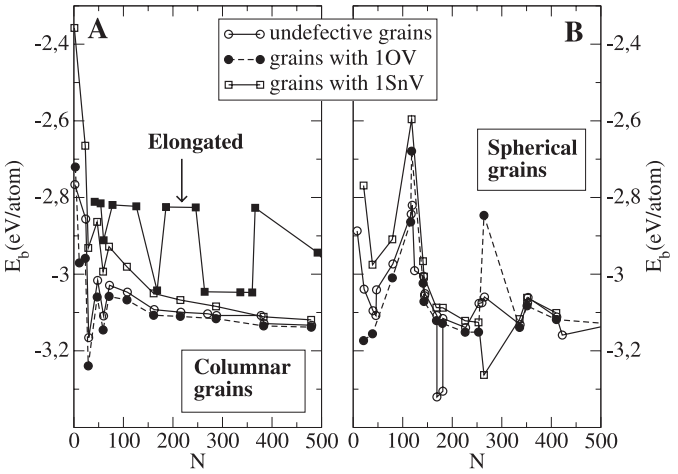

Fig. 2. The functional dependence of the binding energy E_b on the grain size (N) and shape. A: columnar grains with either a low a/c or with an appreciable elongation (filled squares). B: spherical grains.

E_b is approximately independent on N. The lattice view in Figure 1 is representative of the shape of the columnar clusters with a size around 40 atoms. The figure shows a large number of boundary atoms whose reduced coordination evidently lowers the grain binding strength with respect to E_c. The constant value of E_b in this group indicates that the increase of E_b due to boundary atoms scales with the grain volume, or area, as $N^{-\alpha}$, where α indicates the rate of growth of the volume, or area, with N. Due to this compensation, the effect of the boundary atoms is almost independent on N and, owing to its $N^{-\alpha}$ dependence, can not be attributed to any particular orbital contribution. Rather, it has to be seen as the result of an effective charge exchange and hybridization.

In contrast with the columnar grains, a weaker and fluctuating binding strength is observed in the spherical and elongated grains. In both cases the structure of the lattice and its composition, rather than the inherent properties of the bonding, are the source of this behaviour. In the spherical grains, due to the carving of the spherical shape, the ratio between the tin and oxygen content is at variance with respect to the optimal value $x = 0.5$ of the rutile lattice, and this produces the observed increase of E_b at the sizes where the change of x is more pronounced. For the elongated grains a plausible count of the boundary atoms is given by a/c. The grains with the higher a/c have also the higher E_b and the oscillatory behaviour of E_b arises from the irregular dependence of N on a/c.

The characterization of a 'defect' in a nanostructure, which is in itself defective with respect to the bulk, is of some subtlety. Known effects of vacancies in crystalline solids are lattice relaxation and special levels in the band structure. For small, point-like defects such as the ones considered in this study, the amount of lattice relaxation is generally limited to an outward/inward relaxation with a length approximatively one tenth of an Å and involves approximately ten locations radially distributed around the vacant lattice site. Conversely, the energy levels are shifted of some tenths of an eV from their normal value. The possible amount of both effects in SnO_2 is suggested by the data on bulk and surfaces reported above. The donor level, associated with an oxygen vacancy, is 0.1 eV below the conduction band minimum. The rumpling of the surface (which can be regarded as a column of regularly bonded atoms with a vacancy on its top) is modest, between 0.1 and 1 Å, and is neutralized by a counter-rumpling in the layers below the surface.

The absence of a proper band structure in the nanograins does not allow the characterization of defects in terms of band structure, though local changes of the structural properties and of electronic charge are certainly produced. The assumptions used in this study allow a separate evaluation of these two effects. The rigid lattice model adopted in TB shows the influence of the defect on the electronic charge. This evaluation is in error by an amount given by the small lattice relaxation mentioned above. These effects are all included in DFT calculations.

In a compound, the primary effect of a vacant lattice site is a change in the stoichiometry, and the effects of a variable stoichiometry is shown by the spherical grains. The effect of vacancies is conceivably similar, i.e. an increase of E_b at the sizes where x, modified by the defect's presence, has a significant change with respect to the bulk value.

The plots of the defective grains in Figure 2 show this to be the case. There are two other important aspects in these calculations. First, the grain lattice contains only one isolated vacancy. However its presence is perceptible even in structures of a relatively large size. This indicates that a strong connectivity is a main feature of the electronic charge of the grain and the presence of even an isolated vacancy lowers the stability of the entire structure. Second, owing to the size dependence of the eigenvalue spectrum, a formation energy, specific of an oxygen or tin vacancy, cannot be identified. Furthermore the E_b plots indicate that the two defects are indistinguishable, while in the bulk a high formation energy is attributed to tin vacancies and these defects, in practice, are not observed [12]. An obvious explanation of this result is that the effect of a vacancy is mediated by the regular bonding in the grain, and is therefore less site-specific than in the bulk. Furthermore, finite-size effects also have to be accounted for. Boundary effects mitigate the difference between the two sublattices such that the properties of their electronic structure are less different than in the bulk. This interpretation is also supported by the fact that the displacement of the vacancy from the grain interior to its surface did not cause any systematic change of E_b.

5 Comparison between TB and DFT. Literature results

The number of literature data relevant for the purposes of this study is extremely limited. They have been collected in Table 2 together with TB and DFT calculations.

The general indication deriving from the comparison of theoretical and experimental results is of a limited accuracy of the latter ones. In the case of oxygen, these effects were first attributed to the failure of the exchange-correlation functionals [25] and recent theories indicate that calculations on SnO_2 critically depend on the choice of the tin potential [24]. However, for small tin clusters, a possible source of disagreement is that some experimental condition, for instance temperature, is not accounted for by the theoretical models. TB calculations favourably compares with other calculations and the differences with respect to experiments fall, on average, within the 10% range. On the contrary, DFT calculations critically depend on the choice of the basis sets and of the potentials. A large overbinding is observed when using LDA, while results within 10–20% with respect to TB and other calculations are obtained with GGC. The spread of the data reported under the entry 'GGC' or 'LDA' arises from the choice of the basis sets, and less accurate results are produced by the more limited sets, like SZ or DZ. However it can not be overlooked that a main cause of this spread is the critical nature of the evaluation of E_b. In fact, the differences among the total energies E_{tot} obtained for a given cluster are limited to a few percent for

Table 3. Comparison of TB and DFT calculations. Rigid lattice model.

grain size N	binding energy E_b [eV/atom]	grain structure
TB calculations		
12–24	–2.86	Columnar ($x = 0.50$)
48	–3.10	”
40	–3.09	Spherical ($x = 0.54$)
80	–2.97	” ($x = 0.48$)
DFT calculations-GGC		
12	–2.97	Columnar($x = 0.50$)
12-1OV	–2.60	” ($x = 0.57$)
24	–3.21	” ($x = 0.50$)
24-1OV	–2.24	” ($x = 0.54$)
48	–3.62	” ($x = 0.50$)
40	–3.46	Spherical ($x = 0.54$)
40-1OV	–3.00	” ($x = 0.56$)
80	–2.89	” ($x = 0.48$)

all simulation conditions. These differences are amplified by the use of E_b, which is the difference between E_{tot} for the cluster and for the free atoms. The evaluation of the structural properties is evidently less critical than that of E_b and the results on these quantities are regularly converging.

DFT calculations of grains using GGC (Tab. 3), in addition to a qualitative agreement with TB, enforce the properties discussed in the previous section, i.e. the nearly flat asymptote in the E_b-vs.-N curves, and the increase of E_b due to an x value diverging from the ideal value of 0.5. Furthermore the study of the relaxed lattice using DFT showed two important features. First, the relaxation leads to a downward shift of E_b of approximately 0.5–0.7 eV/atom and, for the limited range of sizes considered in DFT calculations, this effect is scarcely dependent on N. Therefore the plots in Figure 2, based on an unrelaxed lattice model, give an accurate relative (if not absolute) evaluation of E_b. Second, the lattice reconstruction consists of irregular displacements. This applies to both boundary atoms and to atoms surrounding a vacancy and is consistent with experiments [29], whereas other DFT calculations of oxygen vacancies show systematic displacements of the tin atoms towards the vacancy and of the oxygen atoms away from it [29]. Owing to the random character of the displacements obtained by DFT, the shape of the grains is retained, at least in its gross form, and this confirms the validity of the rigid lattice model adopted in TB.

6 Conclusion

To conclude, in this work we have presented an evaluation of the binding energy of SnO_2 grains based on both TB and DFT. In this presentation, particular care has been taken to offer an exhaustive comparison with literature data on the various phases of the material, i.e. bulk, surface and clusters. The calculations show that E_b is a sensitive indicator of the grain structure, composition and of its defective state. The grain stoichiometry appears to be the most critical parameter and its change from the bulk value, produced either intentionally by the carving of the grain shape or due to a vacant lattice site, may lead to a perceptible increase in E_b. This, in turn, endangers the grain stability. DFT calculations show that the effects arising from the relaxation of the grain lattice are weak and fluctuating.

References

1. C.M. Goringe, D.R. Bowler, E. Hernandez, Rep. Prog. Phys. **60**, 1447 (1997)
2. J. Robertson, J. Phys. C: Solid State Phys. **12**, 4753 (1979), J. Robertson, J. Phys. C: Solid State Phys. **12**, 4767 (1979)
3. T.J. Godin, J.P. LaFemina, Phys. Rev. B **47**, 6518 (1993)
4. G. Calzaferri, L. Forss, I. Kamber, J. Phys. Chem. **93**, 5366 (1989)
5. J.M. Soler, E. Artacho, J.D. Gale, A. Garcia, J. Junquera, P. Ordejon, D. Sanchez-Portal, J. Phys.: Condens. Matter **14**, 2745 (2002)
6. J. Goniakowski, J.M. Holender, L.N. Kantorovich, J.M. Gillan, J.A. White, Phys. Rev. B **53**, 957 (1996)
7. Wang Dazhi, Wen Shulin, Chen Jun, Zheng Suyuan, Li Fangqing, Phys. Rev. B **49**, 14282 (1994)
8. K.M. Yu, Y. Xiong, Y. Liu, C. Xiong, Phys. Rev. B **66**, 2666 (1997)
9. A. Parisini, R. Angelucci, L. Dori, A. Poggi, P. Maccagnani, G.C. Cardinali, G. Amato, G. Lerondel, D. Midellino, Micron **31**, 223 (2000)
10. A.M. Mazzone, Comp. Mat. Sci. **21**, 211 (2001)
11. A.M. Mazzone, Phil. Mag. Lett. **82**, 99 (2002), ibid. **84**, 275 (2004)
12. S. Munnix, M. Schmeits, Phys. Rev. B **33**, 4136 (1986)
13. B.K. Panda, S. Mukherjee, S.N. Behera, Phys. Rev. B **63**, 45404 (2001)
14. G. Tomassini, M.G. Selme, P. Pecheur, Phys. Rev. B **36**, 6135 (1987)
15. P.K. Schelling, N. Yu, J.W. Halley, Phys. Rev. B **58**, 1279 (1998)
16. L.J. Munro, D.J. Wales, Phys. Rev. B **59**, 3969 (1999)
17. L.A. Grunes, R.D. Leapman, C.N. Wilker, R. Hoffmann, A.B. Kunz, Phys. Rev. B **25**, 7157 (1982)
18. J.K. Burdett, Inorg. Chem. **24**, 2244 (1985)
19. E.L. Peltzer Blanca', A. Svane, E. Christensen, C.O. Rodriguez, O.M. Capannini, M.S. Moreno, Phys. Rev. B **48**, 15712 (1993)
20. J. Terra, D. Guenzburger, Phys. Rev. B **114**, 8584 (1991)
21. D.Le. Bellac, J.M. Kiat, P. Garnier, J. Solid. State Chem. **114**, 459 (1995)
22. G.W. Watson, J. Chem. Phys. **114**, 758 (2001)
23. J.R. Chelikowsky, D.J. Chadi, M. Biggeli, Phys. Rev. B **64**, R2051 (2000)
24. M. Meyer, G. Onida, M. Palummo, L. Reining, Phys. Rev. B **64**, 45119 (2001)
25. G.S. Painter, F.W. Averill, Phys. Rev. B **26**, 1781 (1982)
26. J. Andezelm, N. Russo, D.R. Salahub, J. Chem. Phys. **87**, 6562 (1987)
27. G. Meloni, R.W. Schmude Jr., J.E. Kingcade, K.A. Gingerich, J. Chem. Phys. **113**, 1852 (2000)
28. Z.Y. Lu, C.Z. Wang, K.-M. Ho, Phys. Rev. B **61**, 239 (2000)
29. J. Oviedo, M.J. Gillan, Surf. Sci. **513**, 26 (2002)